3D numerical modelling of earth pressures on a non-yielding rigid wall due to compaction efforts

Islam Ezzeldin, Hany El Naggar and John Newhook

Department of Civil and Resource Engineering, Dalhousie University, Nova Scotia, Canada

ABSTRACT

This paper investigates the simulation of the impact of compaction efforts on buried non-yielding rigid structures utilizing three-dimensional finite element models. The model presents the impact of a five-lift compaction process on a rigid wall that was tested in the laboratory facility at the National Chiao Tung University (NCTU) in Taiwan. The numerical modelling results are validated with measurements from the experimental data. The numerical analysis simulates the backfill soil material via three commonly used material models: the linear elastic (LE), Mohr-Coulomb (MC), and hardening soil (HS) models. The results of the 3D modelling show that the HS model estimates the soil response to backfilling efforts more efficiently than the other material models. Moreover, this study suggests two techniques for simulating the compaction efforts for compacting and densifying the soil from the loose state to the compacted dense state: by using surface pressure loading, or prescribed surface displacements.

Key words: Compaction, numerical modelling, rigid wall, earth pressure, backfill.

RÉSUMÉ

Cet article examine l'impact de la simulation des efforts de compactage en appliquant la modélisation numérique 3D sur les structures rigides non cédantes enfouies. Le modèle actuel est réalisé pour simuler le processus de compactage de cinq ascenseurs sur une installation à paroi rigide à l'Université nationale Chiao Tung (NCTU) à Taïwan. Les résultats numériques sont validés avec les mesures réelles des données expérimentales. L'analyse numérique a simulé le matériau du sol de remblayage en utilisant trois modèles de matériaux courants : élastique linéaire (LE), Mohr-Coulomb (MC) et sol durcissant (HS). Les résultats du modèle 3D montrent l'efficacité de l'utilisation du modèle SH pour estimer la réponse du sol aux efforts de remblayage par rapport à d'autres modèles de matériaux. De plus, cette étude suggère deux techniques pour simuler l'effort de compactage en utilisant les charges de pression de surface et les déplacements de surface prescrits pour compacter et densifier le sol de l'état lâche à l'état dense compacté.

Mots clés : Compaction, modélisation numérique, paroi rigide, pression de la terre, remblayage.

1. INTRODUCTION

The process of compacting backfill soil behind buried structures during construction plays a vital role in the performance of the entire soil-structure system (Wadi et al., 2020). The backfilling mechanism is considered to be one of the most important methods for stabilizing the soil and improving existing soil fills (Chen and Fang, 2008). The main objective of compacting the soil surrounding buried structures is to provide adequate confinement in order to increase the soil strength and decrease the corresponding settlement (Ezzeldin and El Naggar, 2021a). The behaviour of the interaction between fills and structures due to compaction efforts is primarily based on the type of structure (i.e., rigid or flexible), the relative stiffness, the backfill properties, and the compaction energy for the planned degree of compaction (Ezzeldin and El Naggar, 2021b). For granular cohesionless backfills, a high relative density is recommended, e.g., greater than 75%, based on the project specifications (US Navy, 1982).

Conventionally, the distribution of earth pressures behind buried structures can be determined based on structure deformations. The pressures can lie in the Rankine active zone when the structure moves in the direction of the soil, in the Rankine passive zone when the movement is in the opposite direction, or in the Jaky at-rest zone when the structure is fully fixed. As described in the literature, the Jaky formula for calculating the at-rest earth pressure can contribute to a good estimate of the earth pressure in loose sands (Sherif et al., 1984). However, to investigate the impact of compaction, research based on laboratory and field studies has provided empirical and analytical approaches for defining formulas for additional lateral earth pressure (Duncan and Seed, 1986, Ingold, 1986, and Peck and Mesri, 1987). Ingold (1986) has determined that the vibratory impact of a compaction roller behind a rigid vertical retaining wall is equivalent to five or six times the effective deadweight of the roller.

Various techniques can be used to simulate compaction efforts, such as hand calculations or finite element analyses (FEA). Numerically, the design of buried

structures relies on factors such as the soil properties before and after compaction, the characteristics of the compaction rollers used, and the methodology employed to simulate the compaction force. Finite element methods are generally recommended in order to incorporate all of the model elements, to investigate the soil-structure response.

This paper investigates 3D numerical simulation of the compaction process, for a non-yielding rigid retaining wall. The numerical modelling is validated with the results of a laboratory test of the compaction impact during backfilling of granular sandy soil in a metal facility. The analysis investigates three commonly used material models: linear elastic (LE), Mohr-Coulomb (MC), and hardening soil (HS) models. In addition, two techniques are defined for simulating the compaction effort: surface pressure loading, and prescribed surface displacement.

2. FULL-SCALE TEST OF EARTH PRESSURE DISTRIBUTION DUE TO VIBRATORY COMPACTION

A laboratory experiment was performed to investigate the impact of the compaction process on an instrumented non-yielding rigid wall at National Chiao Tung University (NCTU) in Taiwan (Chen and Fang, 2008). The laboratory model had three main components: a rigid retaining wall to capture the data, a soil bin, and a data acquisition system. The soil bin, made of solid steel plates, had a total height of 1.6 m and a square cross-section measuring 1.5 m x 1.5 m. The retaining wall thickness was 45 mm, and the thickness of the side and end walls was 35 mm. To achieve full rigidity of the model wall with the backfill at rest behind it, the wall and soil bin were surrounded by 12 channel section steel beams and 24 vertical steel columns with a thickness of 20 mm. All the structural elements of the model were welded together to increase the model stiffness by providing fixities, thus preventing lateral deformations during the backfilling process or during the application of external loads. Soil pressure transducers were placed at the model wall to investigate the earth pressure distribution, with 15 transducers to measure the vertical earth pressure and 15 to measure the horizontal earth pressure. Figure 1 shows the model set-up with the rigid retaining model wall and the soil bin, and Figure 2 illustrates the positioning of the soil pressure transducers.

The backfill soil used was air-dry Ottawa sand, with a specific gravity of 2.65, D_{60} = 0.39 mm, D_{10} = 0.26 mm, e_{max} = 0.76, and e_{min} = 0.5. The relative density of the soil was 32% in a loose state before compaction, and 75% in a dense state after compaction. The soil was compacted in five lifts with an average thickness of 300 mm after compaction. The vibratory compactor had a total mass of 12.1 kg, with a steel plate base measuring 225 mm x 225 mm x 2 mm.

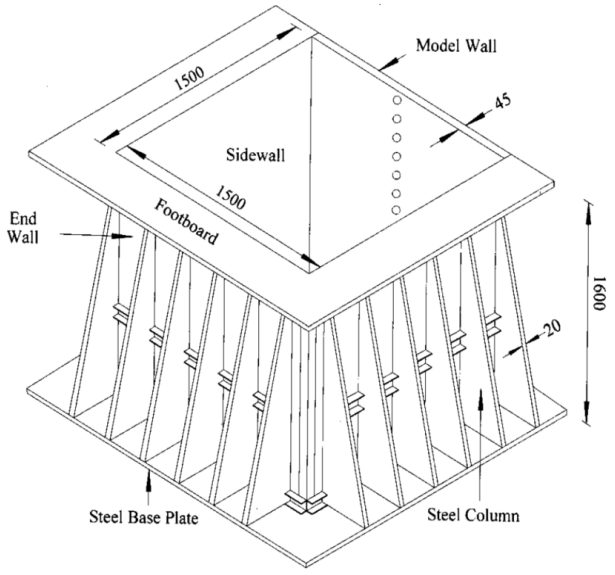

Units (mm)

Figure 1. Model set-up with non-yielding rigid retaining wall, at NCTU (Chen and Fang, 2008)

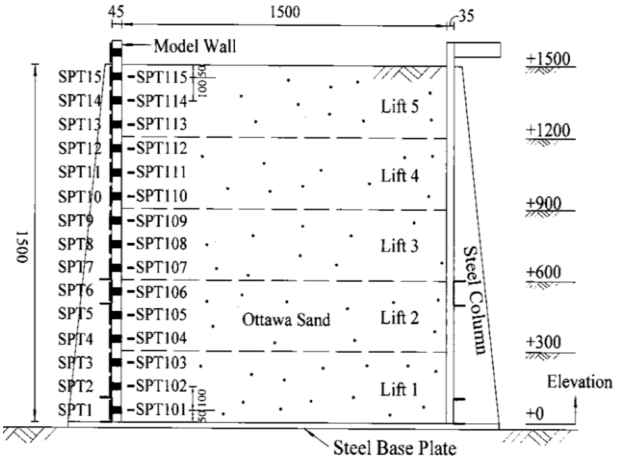

Units (mm)

Figure 2. Positioning of the soil pressure transducers (Chen and Fang, 2008)

3. NUMERICAL ANALYSIS OF THE COMPACTION METHODOLOGY

The numerical modelling of the model retaining wall with the soil bin includes backfilling stages for five lifts, from the level of the base to a height of 1.5 m, as shown in Figure 3. From a loose state with a thickness of around 322 mm, each layer was densified and compacted to a final dense state with an approximate average thickness of 300 mm. Thus, there was a total downward compression of about 22 mm. The numerical modelling was performed with the aid of the PLAXIS 3D finite element program. Interface boundaries were added for the walls and base. In the laboratory experiment, at the model walls, a layer of one thick and two thin plastic sheets was installed to minimize any friction between the soil and the walls. To simulate this,

an interface boundary with a very minimal interface reduction coefficient ($R_{int.}$=0.01) was defined in the numerical model. In contrast, the base of the soil bin was covered with a layer of safety walk material, to provide adequate friction between the soil and the base of the bin. To simulate this, another interface boundary with a fully rigid interface coefficient ($R_{int.}$=1.0) was defined in the numerical model. In the numerical modelling, standard fixities were defined around the model wall boundaries to fix the model in the X and Y directions. In the Z direction, the upper surface was set to be free, with frictionless side interfaces to permit deformation. Very fine meshing was selected, with around 240000 elements, an average mesh size of 49 mm, and approximately 401000 nodes, as illustrated in Figure 4.

The backfill soil layers were modelled in the loose state before compaction, and in the dense state after compaction. To model the backfill compaction efforts and determine the response at the rigid retaining wall, the soil material was modelled by employing three commonly used constitutive models: the linear elastic (LE) material model, the Mohr-Coulomb (MC) material model, and the hardening soil (HS) material model. In the LE model, the soil is simulated as an elastic material in accordance with Hooke's law of elasticity; in the MC model, the soil behaves as an elastic-plastic material; and in the HS model the soil is defined as a yield surface, with expansion potential due to plastic straining (PLAXIS 3D, 2021). Table 1 presents characteristics of the backfill soil in the loose and dense states, for the three material models. In simulating the backfilling process, compaction was simulated by using two methods suggested by Ezzeldin and El Naggar (2022): the surface pressure loading method, and the prescribed surface displacement method. To simulate each lift, first the backfill layer was activated in the loose state with its associated surface pressure or prescribed surface displacement. Then the loose layer was converted into a dense layer, with deactivation of its previous surface pressure loading or prescribed surface displacement. Subsequently, the next lift was activated in the loose state with its new surface pressure loading or prescribed surface displacement. This procedure was repeated until the end of backfilling. The impact of the vibratory compactor was measured in situ as applying a surface pressure of 34.9 kPa. However, this value is greatly overestimated in terms of the numerical modelling and also as compared to the range suggested by Ingold (1986) for rigid structures (i.e., a cyclic impact of around five to six times the compactor deadweight). Thus, in the analysis, a surface pressure load of around 14 kPa was used (determined from the static compactor weight added to the static compactor weight multiplied by five, i.e., 2.34 kPa + [5 x 2.34 kPa] = 14.04 kPA). For the prescribed displacement, a value of 2.2 mm, equivalent to about 10% of the total displacement, was used to simulate the compaction impact, as suggested by Ezzeldin and El Naggar (2022). Figure 5 illustrates three sequential stages of backfill compaction used in the numerical model.

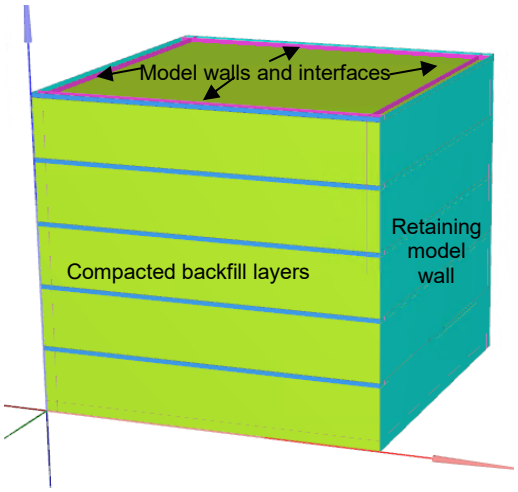

Figure 3. Illustration of the backfill layers used in numerical modelling of the model retaining wall

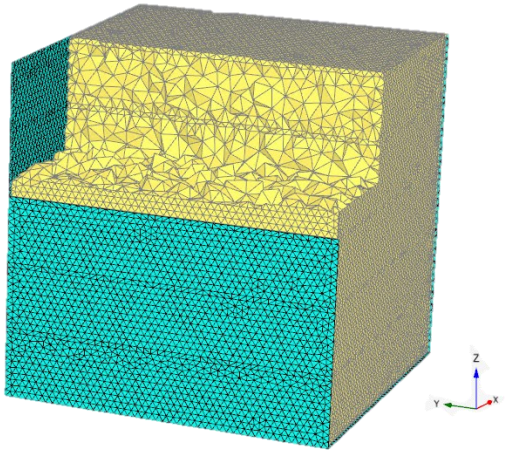

Figure 4. Illustration of numerical model meshing for the model retaining wall and soil bin

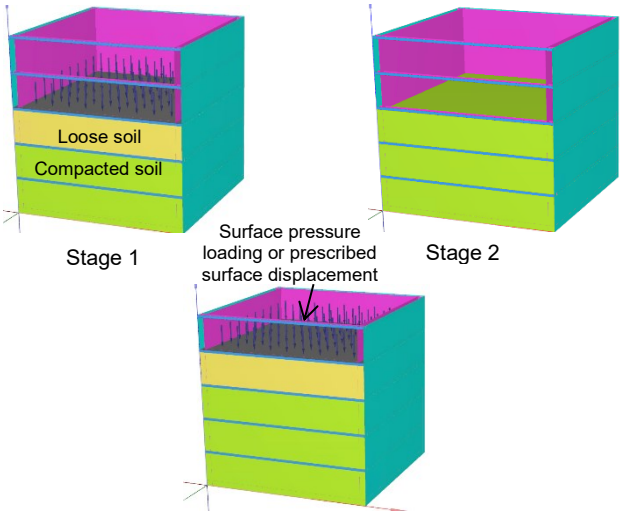

Figure 5. Three sequential stages of backfill compaction used in the numerical model

Table 1. Characteristics of the backfill soil in the loose and dense states, for the three material models

Soil Characteristics	**Loose Backfill Soil**		
Material model	LE	MC	HS
Soil density (γ) (kN/m^3)	15.50	15.50	15.50
Modulus of elasticity (E) = E_{50} (Mpa)	10.75	10.75	10.75
$E_{oedemeter}$ (MPa)	_	_	10.75
$E_{unloading\text{-}reloading}$ (MPa)	_	_	32.25
Poisson's ratio (υ)	0.20	0.20	0.20
Cohesion (c) kPa	_	0	0
Friction angle (φ)	_	30.7°	30.7°
Dilatancy angle (Ψ)	_	0.7°	0.7°
Soil Characteristics	**Dense Backfill Soil**		
Material model	LE	MC	HS
Soil density (γ) (kN/m^3)	16.60	16.60	16.60
Modulus of elasticity (E) = E_{50} (Mpa)	38	38	38
$E_{oedemeter}$ (MPa)	_	_	38
$E_{unloading\text{-}reloading}$ (MPa)	_	_	114
Poisson's ratio (υ)	0.20	0.20	0.20
Cohesion (c) kPa	_	0	0
Friction angle (φ)	_	40.8°	40.8°
Dilatancy angle (Ψ)	_	10.8°	10.8°

4. RESULTS AND DISCUSSION

In the laboratory, the model retaining wall was monitored during each backfilling stage to record the vertical and horizontal earth pressure. Before compaction efforts were applied, the soil was placed in its loose state, so that differences before and after compaction could be determined. Figure 6 (a) shows the vertical stress distribution of laboratory and numerical modelling results for loose and compacted backfill. Here it can be observed that only the weight of the soil itself is exhibited, based on the soil density, without any additional vertical stresses. Figure 6 (b) shows that for loose backfill, the numerical modelling horizontal stress distribution results agree with the lab tests and are in accordance with Jaky's at-rest formula (i.e., $K_o = 1 - \sin\varphi$).

To investigate the effect of the material model employed, three common material models, i.e., LE, MC and HS models, were used to simulate the compaction efforts. Figure 7 presents the horizontal stress distribution results for the first backfill lift, obtained via the surface pressure loading method. The numerical modelling results show the efficiency of using the HS material model to simulate the behaviour of the backfill soil during compaction. This is illustrated in Figure 7, where the results obtain via the HS model show closer agreement with the laboratory compaction measurements of the horizontal pressures than is the case with the LE and MC model results.

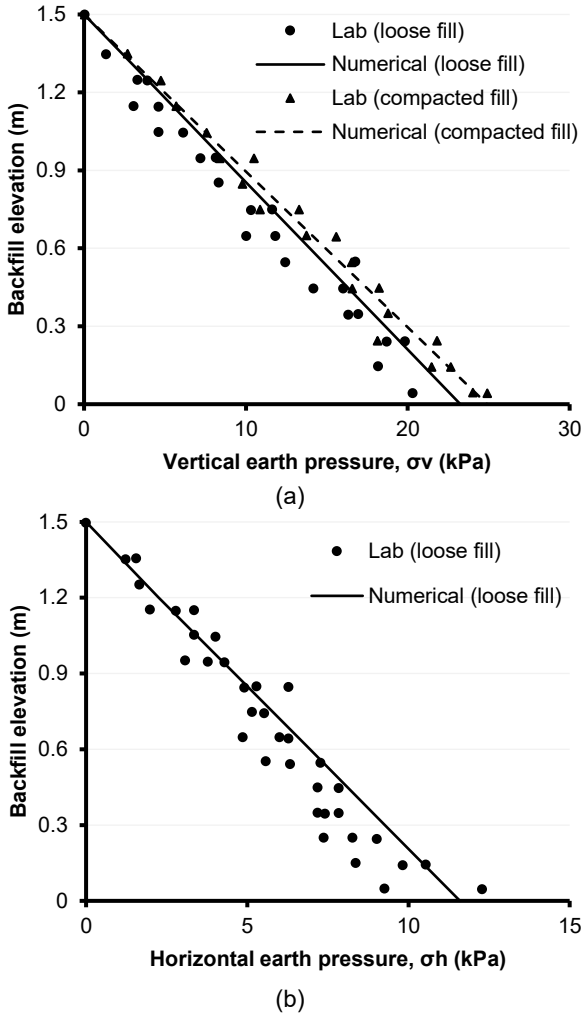

Figure 6. (a) Vertical earth pressure distribution for loose and compacted backfill, and (b) horizontal earth pressure distribution for loose backfill

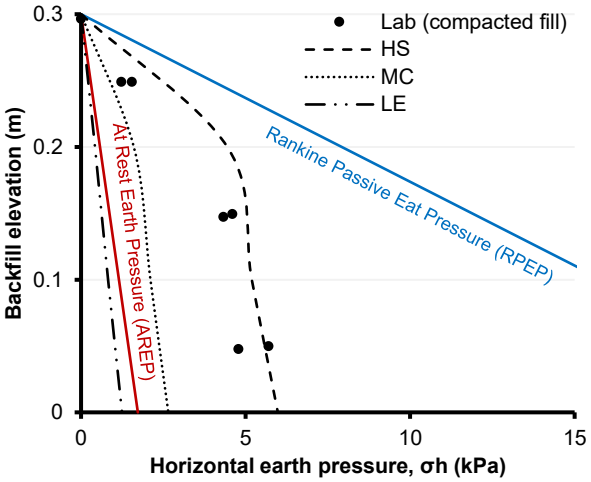

Figure 7. Horizontal earth pressure distributions for the first backfill compaction lift, obtained by using the LE, MC, and HS material models

Numerical simulation of the compaction efforts was performed by using the surface pressure loading method and the prescribed surface displacement method. In Figure 8, the horizontal earth pressure distribution after compaction is plotted for each backfill lift until the end of backfilling. Two laboratory compaction tests were performed to measure the soil performance. Figure 8 shows that for most of the results, the lab measurements lie between Jaky's at-rest earth pressure (AREP) and the Rankine passive earth pressure (RPEP). This is in good agreement with the numerical modelling horizontal earth pressure results obtained by using both compaction simulation methods. However, at a few points, the lab horizontal earth pressure results tend toward the passive estimates. This might be attributable to a kneading impact on the soil, where compaction loads due to more rounds or increased compaction time could result in applied stresses that exceed the soil bearing capacity. For the final two backfill lifts, it was also found that the horizontal earth pressures at the bottom layers tended to be lower than the at-rest pressures. This might be attributable to some movement of the soil bin, which could reduce the applied horizontal stresses.

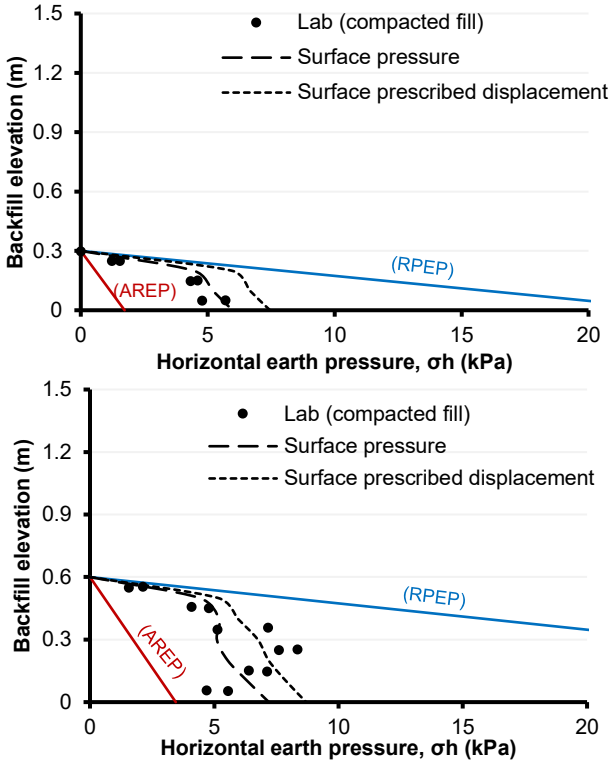

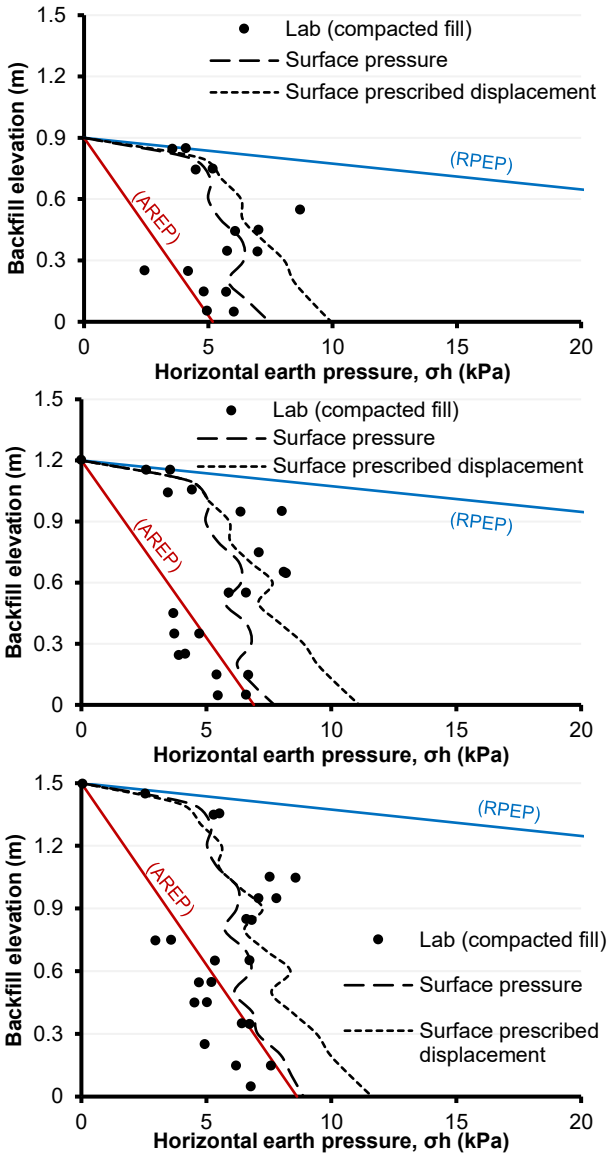

Figure 8. Horizontal earth pressure distributions after compaction of each backfill lift, simulated via surface pressure loading and prescribed surface displacement

5. CONCLUSION

This paper presents 3D numerical modelling of compaction efforts on backfill behind a rigid non-yielding retaining wall. Numerical modelling was performed by using the finite element software PLAXIS 3D to capture the soil performance during loading. Three commonly used material models were employed to simulate the backfill behaviour. It is concluded that the performance exhibited by the HS model in simulating soil under compaction loading was superior to that of the LE and MC models. Furthermore, the simulation of compaction via surface pressure loading and prescribed surface displacement methods was found to give good agreement with laboratory measurements of horizontal earth pressures in compacted soil behind a model rigid retaining wall.

7. REFERENCES

Chen, T. J., and Fang, Y. S. (2002). “A new facility for measurement of earth pressure at-rest.” *Geotech. Eng.*, 333, 153–159.

Chen, T. and Fang, Y. (2008). “Earth Pressure due to Vibratory Compaction.”, Journal of Geotechnical and Geoenvironmental Engineering.

Duncan, J. M., and Seed, R. B. (1986). “Compaction-induced earth pressure under K_o-conditions.” J. Geotech. Eng., 112(1), 1–22.

Ezzeldin, I. and El Naggar, H. (2021a). “Three-dimensional finite element modeling of corrugated metal pipes.”, *Transportation Geotechnics*, Volume 27.

Ezzeldin, I. and El Naggar, H. (2021b). “Earth pressure distribution around flexible arch pipes.”, *Engineering Structures,* Volume 237.

Ezzeldin, I. and El Naggar, H. (2022). “Numerical Modelling of Induced Stresses in Buried Corrugated Metal Structures due to Compaction Efforts.”, Transportation Geotechnics, Volume 32, 2022, 100706, ISSN 2214-3912.

Ingold, T. S. (1986). Discussion of "Compaction-induced earth pressure under K_o-conditions." J. Geotech. Engrg., 113(11): 1403-1405.

Peck, R. B., and Mesri, G. (1987). “Discussion of "Compaction-induced earth pressure under K_o-conditions." J. Geotech. Engrg., 113(11): 1406-1408.

PLAXIS 3D. (V2021), Reference Manual.

PLAXIS 3D. (V2021), Material Model Manual.

Sherif, M. A., Fang, Y. S., and Sherif, R. I. (1984). “*Ka* and *Ko* behind rotating and nonyielding walls.” *J. Geotech. Engrg.*, 1101, 41–56.

US Navy. (1982). “*Foundations and earth structures, NAVFAC design manual DM-7.2”*, Washington, D.C.

Wadi, A., Pettersson, L., and Karoumi, R. (2020). “On Predicting the Ultimate Capacity of a Large-Span Soil–Steel Composite Bridge.”, International Journal of Geosynthetics and Ground Engineering, 6 (4), 48.